THE JOURNAL OF BIOLOGICAL CHEMISTRY VOL. 285, NO. 43, pp. 33054–33064, October 22, 2010

Novel Inhibitors of *Plasmodium falciparum* Dihydroorotate Dehydrogenase with Anti-malarial Activity in the Mouse Model*[S]

Received for publication, July 9, 2010, and in revised form, August 3, 2010 Published, JBC Papers in Press, August 11, 2010, DOI 10.1074/jbc.M110.162081

Michael L. Booker,[a1] Cecilia M. Bastos,[a] Martin L. Kramer,[a] Robert H. Barker, Jr.,[a] Renato Skerlj,[a] Amar Bir Sidhu,[b] Xiaoyi Deng,[c] Cassandra Celatka,[a] Joseph F. Cortese,[b] Jose E. Guerrero Bravo,[d] Keila N. Crespo Llado,[d] Adelfa E. Serrano,[d] Iñigo Angulo-Barturen,[e] María Belén Jiménez-Díaz,[e] Sara Viera,[e] Helen Garuti,[e] Sergio Wittlin,[f,g] Petros Papastogiannidis,[f,g] Jing-wen Lin,[h] Chris J. Janse,[h] Shahid M. Khan,[h] Manoj Duraisingh,[i] Bradley Coleman,[i] Elizabeth J. Goldsmith,[j] Margaret A. Phillips,[c2] Benito Munoz,[b] Dyann F. Wirth,[i] Jeffrey D. Klinger,[a] Roger Wiegand,[b] and Edmund Sybertz[a]

From [a]Genzyme Corporation, Waltham, Massachusetts 02451, the [b]Broad Institute of Harvard and MIT, Cambridge, Massachusetts 02141, the [d]Department of Microbiology and Medical Zoology, University of Puerto Rico School of Medicine, P. O. Box 365067, San Juan, Puerto Rico 00936-5067, the [e]Medicines Development Campus, Diseases of the Developing World, GlaxoSmithKline, c/Severo Ochoa 2, 28760 Tres Cantos, Spain, the [f]Swiss Tropical and Public Health Institute, Socinstrasse 57, CH-4002, Basel, Switzerland, the [g]University of Basel, Petersplatz 1, CH-4003, Basel, Switzerland, the [h]Leiden Malaria Research Group, Department of Parasitology, Centre for Infectious Diseases, Leiden University Medical Center, 2333 ZA Leiden, The Netherlands, the [i]Department of Immunology and Infectious Diseases, Harvard School of Public Health, Boston, Massachusetts 02115, and the Departments of [c]Pharmacology and [j]Biochemistry, University of Texas Southwestern Medical Center, Dallas, Texas 75390-9041

***Plasmodium falciparum*, the causative agent of the most deadly form of human malaria, is unable to salvage pyrimidines and must rely on *de novo* biosynthesis for survival. Dihydroorotate dehydrogenase (DHODH) catalyzes the rate-limiting step in the pyrimidine biosynthetic pathway and represents a potential target for anti-malarial therapy. A high throughput screen and subsequent medicinal chemistry program identified a series of *N*-alkyl-5-(1H-benzimidazol-1-yl)thiophene-2-carboxamides with low nanomolar *in vitro* potency against DHODH from *P. falciparum*, *P. vivax*, and *P. berghei*. The compounds were selective for the parasite enzymes over human DHODH, and x-ray structural data on the analog Genz-667348, demonstrated that species selectivity could be attributed to amino acid differences in the inhibitor-binding site. Compounds from this series demonstrated *in vitro* potency against the 3D7 and Dd2 strains of *P. falciparum*, good tolerability and oral exposure in the mouse, and ED_{50} values in the 4-day murine *P. berghei* efficacy model of 13–21 mg/kg/day with oral twice-daily dosing. In particular, treatment with Genz-667348 at 100 mg/kg/day resulted in sterile cure. Two recent analogs of Genz-667348 are currently undergoing pilot toxicity testing to determine suitability as clinical development candidates.**

Malaria is currently one of the world's most severe endemic diseases, and, despite the advent of combination therapy and the introduction of longer acting pharmaceuticals, the need for new targets and relevant anti-malarial agents remains acute. DHODH,[3] the enzyme catalyzing the fourth and rate-limiting step in *de novo* pyrimidine biosynthesis, represents a potential biological target that could be exploited. Pyrimidines are required for the biosynthesis of DNA, RNA, glycoproteins, and phospholipids. Unlike the human host, *P. falciparum* lacks the ability to salvage pyrimidine bases and thus is entirely dependent on *de novo* biosynthesis (1, 2). DHODH catalyzes the oxidation of L-dihydroorotate to orotate via a coupled redox reaction with a bound flavin cofactor (3–6). DHODH is ubiquitous to most organisms and exists in two forms. The cytosolic Type 1 enzyme is present in Gram-positive bacteria and *Saccharomyces cerevisiae* and utilizes fumarate or NAD^+ as an electron acceptor (4, 7–10). The membrane-bound Type 2 enzyme is present in eukaryotes and some Gram-negative bacteria (11–14) and utilizes quinones as electron acceptors (15). The eukaryotic enzyme, including the plasmodial form, is localized to the inner mitochondrial space and uses coenzyme Q (16–19). The crucial nature of the reaction catalyzed by *Pf*DHODH is reflected in the fact that, during the intra-erythrocytic stages of *P. falciparum* development, the sole function of mitochondrial electron transport appears to be regeneration of coenzyme Q as a cofactor for DHODH (20).

Significant differences between the plasmodial and human enzymes are suggested by previous studies with A77 1726, the

* This work was supported, in whole or in part, by National Institutes of Health Grants U01AI075594 and AI053680 (to M. A. P.). This work was also supported by the Medicines for Malaria Venture and the Humanitarian Assistance for Neglected Diseases Initiative of Genzyme Corp.

The atomic coordinates and structure factors (code 3O8A) have been deposited in the Protein Data Bank, Research Collaboratory for Structural Bioinformatics, Rutgers University, New Brunswick, NJ (http://www.rcsb.org/).

[S] The on-line version of this article (available at http://www.jbc.org) contains supplemental Table 1S.

[1] To whom correspondence should be addressed: Genzyme Corp., 153 Second Ave., Waltham, MA 02451. Tel.: 781-434-3432; Fax: 781-466-3789; E-mail: michael.booker@genzyme.com.

[2] Supported by the Welch Foundation (Grant I-1257). Holds the Carolyn R. Bacon Professorship in Medical Science and Education.

[3] The abbreviations used are: DHODH, dihydroorotate dehydrogenase; *Pf*DHODH, *P. falciparum* DHODH; DHO, dihydroorotate; CoQ, coenzyme Q; *Pf*DHODH-348, the x-ray structure of *Pf*DHODH bound to Genz-667348; DSM1, 5-methyl-[1,2,4]triazolo[1,5-*a*]pyrimidin-7-yl)naphthalen-2-yl-amine; A77 1726, 2-cyano-3-hydroxy-*N*-[4-(trifluoromethyl)phenyl]-2-butenamide; hERG, human Ether-a-go-go Related gene.

active metabolite of the immunomodulatory drug leflunomide. Differences in the sequence and alignment of residues in the region of the inhibitor-binding site have been demonstrated for the parasite and human enzymes complexed with A77 1726 and orotate (21, 22) and a recently reported triazolopyrimidine series of *Pf*DHODH-selective inhibitors (23). Furthermore, A77 1726 has been shown to be a preferential inhibitor of the human enzyme with only weak activity against the parasite enzyme (24). These results support the likelihood of finding inhibitors specific for *Pf*DHODH, and combined with the essential nature of this enzyme in the parasite, establish it as a potentially viable and relevant anti-malarial chemotherapeutic target. In fact, small molecule inhibitors of *Pf*DHODH have previously been described, which demonstrate *in vitro* activity against cultured strains of *P. falciparum* (25, 26) as well as suppression of parasite growth in an animal model (27).

This report describes current lead compounds from an ongoing medicinal chemistry program that represent analogs of progenitor molecules previously identified as inhibitors of *Pf*DHODH (25). The enzyme assays were expanded to include DHODH from *P. berghei* and *P. vivax*, and parasite viability assays were performed not only on *P. falciparum* but also on *P. knowlesi* as an initial step toward discovering compounds with potential pan-species activity. The correlation between inhibitory potency against the enzyme and toxicity toward the parasite was assessed. *In vitro* and *in vivo* drug absorption, distribution, metabolism, and excretion properties were evaluated, and compound efficacy was assessed in the *P. berghei* and *P. falciparum* NOD-*scid* mouse models.

EXPERIMENTAL PROCEDURES

DHODH Inhibition Assays—DHODH plasmid construction, protein expression and purification, and the initial high throughput screen and its results have been previously described (25). The DHODH activity assay monitored the reduction of 2,6-dichloroindophenol and was conducted in 50 μl of 100 mM HEPES (pH 8.0) containing 150 mM NaCl, 5% glycerol, 0.05% Triton X-100, 175 μM L-dihydroorotate, 18 μM decylubiquinone, and 95 μM 2,6-dichloroindophenol, arrayed in a 384-well format. The concentrations of enzymes used were as follows: *P. falciparum*, 12.5 nM, *P. berghei*, 25.5 nM, *P. vivax*, 19.5 nM, and human, 7 nM. Following a 20-min incubation at room temperature, the absorbance was measured at 600 nm (Envision, PerkinElmer Life Sciences). A sigmoidal dose-response curve was generated by plotting % inhibition as a function of the log of compound concentration (range: 1.5 nM to 30 μM), and an IC_{50} value representing the concentration at which inhibition was half-maximal was determined.

Expression and Purification of P. falciparum DHODH for Crystallography—Previously, the Phillips laboratory reported that deletion of a surface loop in *Pf*DHODH containing amino acid residues 384–413 facilitated crystallization of the enzyme with the triazolopyrimidine class of inhibitors (23). This construct also contains an N-terminal deletion that removes the mitochondrial membrane-spanning domain as well as residues that are N-terminal to this region. However, the described construct, pET-*pf*$DHOD_{\Delta 384-413}$, did not routinely yield good quality co-crystals for inhibitors from other structural classes. The construct was redesigned to shorten the N-terminal tag by replacement of the thrombin site and T7 tag sequence with the TEV protease site. pET28b (Novagen) was digested with Nco1/BamH1 and ligated to the annealed oligomer pairs 1 and 2 containing the TEV protease site to generate pET28b-TEV: 1 (CATGGGCCATCACCATCACCATCACGCTGAGAATC-TTTATTTTCAGGGCGCG) and 2 (GATCCGCGCCCT-GAAAATAAAGATTCTCAGCGTGATGGTGATGGTGAT-GGCC). The DNA-encoding *Pf*$DHODH_{\Delta 384-413}$ was isolated by BamH1/Sal1 digestion of pET-*pf*$DHOD_{\Delta 384-413}$ (23) and ligated with the BamH1/Sal1 fragment of pET28b-TEV to generate the final expression construct pET28b-TEV-*pf*$DHOD_{\Delta 384-413}$. This construct yielded protein that could more consistently be crystallized with a wider range of inhibitors than pET-*pf*$DHOD_{\Delta 384-413}$. pET28b-TEV-*pf*$DHOD_{\Delta 384-413}$ was transformed into *Escherichia coli* BL21 phage-resistant cells (Novagen), and *Pf*$DHODH_{\Delta 384-413}$ was expressed and purified as previously described by using HisTrap HP column (Amersham Biosciences) affinity chromatography followed by gel filtration (23).

Crystallization and Data Collection of PfDHODH$_{\Delta 384-413}$ Bound to Inhibitors—Preliminary crystallization conditions were found using the random crystallization screen *Cryo* suite (Nextal) and detergent screen kits (Hampton Research). Subsequently the conditions were refined by variation of pH, precipitant, detergent, and protein concentrations. Crystals of *Pf*$DHODH_{\Delta 384-413}$ were grown by vapor diffusion in a hanging drop at 20 °C. Co-crystals with Genz-667348 were obtained by mixing Reservoir solution A (0.16 M ammonium sulfate, 0.1 M sodium acetate, pH 4.4, 14–15% PEG4000, 25% glycerol, and 10 mM DTT) with an equal volume of *Pf*$DHODH_{\Delta 384-413}$ (20 mg/ml) pre-equilibrated with 0.6 mM Genz-667348 and 2 mM dihydroorotate.

Diffraction data were collected at 100 K on beamline 19ID at Advanced Photon Source using an ADSC Q315 detector. The crystal of *Pf*DHODH-348 diffracted to 2.4 Å and has a space group of $P6_4$ with the cell dimension of a = b = 85.3, c = 138.7, with one molecule of *Pf*DHODH in the asymmetric unit. Diffraction data were integrated, and intensities were scaled with the HKL2000 package (28).

Structure Determination and Refinement of PfDHODH Bound to Inhibitors—Crystallographic phases for *Pf*DHODH inhibitors were solved by molecular replacement with Phaser (29) using the previously reported structure of *Pf*$DHODH_{\Delta 384-413}$ bound to DSM1 (PDB ID 3I65) (23), as a search model. Structures were rebuilt with COOT (30) and refined with REFMAC (31). The phases were improved with DM (32) (Table 1S). The final *Pf*DHODH-348 structure contains residues Phe-161 through Leu-565, one molecule of FMN, orotate, Genz-667348, and 37 water molecules. The structure was refined to R_{fac} of 0.20 and R_{free} of 0.23 (Table 1S). A Ramachandran plot generated with Molprobity (33) indicated that 97.3% of all protein residues are in the most favored regions with the remaining 2.7% in allowed regions. Water molecules were added if the density was stronger than 3.4 σ and removed if the density was weaker than 1 σ in the density map generated with ARP/warp (34).

Molecular Modeling—Structures were displayed using the graphics program PyMOL (56). The *Pf*DHODH/Genz-667348

structure was superimposed with the *Pf*DHODH-DSM1 (PDB 3I65), *Pf*DHODH-A77 1726 (PDB 1TV5), and human DHODH bound to brequinar (*Hs*DHODH-Bre, PDB 1D3G) structures by aligning the backbone atoms of full-length structures in DaliLite (35). Root mean square deviation values were calculated for the superimposed structures based on the C_α positions with DaliLite.

In Vitro P. falciparum Viability Assay—A SYBR green assay as previously described by Plouffe *et al.* (36) was modified for use in 384-well plates. Briefly, parasites were cultured in the presence of serial dilutions of test compounds in 50 μl of RPMI containing 4.16 mg/ml Albumax at a 2.5% hematocrit and an initial parasitemia of 0.3% in black Greiner GNF clear-bottom plates. Following a 72-h incubation at 37 °C under 93% N_2, 4% CO_2 and 3% O_2, SYBR green was added to a dilution of 1:10,000, and plates were stored overnight (or until ready to be read) at −80 °C. Plates were centrifuged at 700 rpm prior to fluorescence measurement (EX 480 nm, EM 530 nM). In this assay, inhibition of parasite replication is reflected in a reduction in the fluorescence intensity of SYBR green bound to parasite DNA.

In Vitro P. knowlesi Viability Assay—Selected compounds were tested against *P. knowlesi* parasites cultured in Rhesus blood cells as a surrogate for *P. vivax* infections using the method of Kocken *et al.* (37). Briefly, *P. knowlesi* were cultured in 2% Rhesus macaque erythrocytes (New England Primate Research Center) in RPMI culture media supplemented with 10% Human O+ serum (Interstate Blood Bank). Schizont stage parasites were purified by flotation in 60% Percoll (GE Life Sciences) and allowed to reinvade to generate a synchronous population of ring stage parasites. Drug assays were performed by plating ring stage parasites at 0.5% parasitemia in triplicate, in RPMI containing 2.5 μg/ml hypoxanthine. Parasites were incubated for 24 h with serially diluted test compounds. After 24 h, thin smears were made to confirm that reinvasion had occurred and 0.5 μCi of ^{3}H-labeled hypoxanthine were added to each well, and parasites were allowed to progress through S-phase to early schizonts. Cells were then harvested via glass filter plates, and ^{3}H incorporation was measured by scintillation counter. Values were normalized to percentage of no drug controls, and IC_{50} values were generated.

In Vitro P. berghei Viability Assay—To investigate if compound potency against DHODH was similarly evident in rodent malaria parasites, selected compounds were assessed for *in vitro* toxicity against *P. berghei* ANKA using the *in vitro* drug luminescence (ITDL) assay (38). This assay is based on the quantitation of luciferase activity (luminescence) using the Luciferase Assay System Kit® (Promega), detected in blood samples containing transgenic blood stage parasites that express luciferase under the control of the schizont-specific (ama-1) promoter (transgenic parasite RMgm-32; http://www.pberghei.eu/index.php?rmgm = 32). Briefly, ring-stage parasites (39, 40) were cultured for 24 h in serial dilutions of test compounds in 24 well plates. Following centrifugation and removal of supernatant, the cells were lysed by addition of cell culture lysis reagent, after which plates were shaken for 5 min. Luciferase assay substrate was added and luminescence was read for 10 s in a multi-plate reader (Wallac 1420 multilabel counter, PerkinElmer). Measurements were expressed in relative light units (RLU) and represent the average of triplicate samples at each drug dilution.

Mammalian Cytotoxicity—Compounds were tested at 10 dilutions against normal human renal proximal tubule cells (Clonetics #CC-2553) and dermal fibroblasts (NHDF; Clonetics #CC-2509). Cells were incubated with compound for 4 days, until becoming confluent. Viability was then measured using the Alamar Blue assay (TREK Diagnostic Systems), according to the manufacturer's instructions.

Erythrocyte Lysis—Compounds were tested at 10 dilutions against fresh human erythrocytes at 1% hematocrit in Dulbecco's PBS in V-bottomed plates incubated for 24 h at 37 °C. Following incubation, plates were centrifuged 5 min at 2,000 rpm and 50 μl of supernatant was transferred to a fresh flat-bottom plate. The amount of hemoglobin present was determined using the QuantChem Hemoglobin Assay Kit (BioAssay Systems #DIHB-250) according to the manufacturer's recommendations.

In Vitro Pharmaceutical Properties—Solubility was determined using a kinetic method. Briefly, compounds were dissolved in DMSO, diluted to 0.5% in phosphate-buffered saline pH 7.4 (PBS), allowed to equilibrate for 16–24 h, and filtered using a 1.2 μm filter. The concentration was calculated from measurement of absorbance at 254 nm using a 96 well plate UV spectrophotometer.

Passive permeability was measured using the parallel artificial membrane permeation assay (PAMPA). Compound was added to the donor well (pH 6.5 in PBS) which was separated from the acceptor well (pH 7.4 in PBS) by a phospholipid membrane in dodecane. After a 5 h incubation, concentrations were measured in donor and acceptor wells by monitoring UV absorbance from 250–490 nm in order to calculate permeability (41).

Metabolic stability was determined using rat, mouse, and human liver microsomes (BD Gentest) as well as intact hepatocytes (CellzDirect). Test compounds were incubated with microsomes at 0.5 mg protein/ml and NADPH as co-factor, or with hepatocytes at 10^6 cells/ml. Samples were withdrawn after 0, 5, 15, 30, and 45 min (microsomes) or 0, 15, 30, 60, and 120 min (hepatocytes) of incubation for liquid chromatography tandem mass spectrometry (LC-MS/MS) analysis. Half-life was determined by plotting Ln (Peak Area ratio) *versus* time (min). The intrinsic clearance was calculated based on the well-stirred model (42) and expressed as ml/min/kg body weight.

Plasma protein binding was calculated by diluting a 25 mM stock solution in DMSO to 1 μM in plasma, dialyzing for 5 h against PBS (pH 7.4) at 37 °C and determining the concentration remaining in each compartment by LC-MS/MS analysis.

Cytochrome P450 (CYP) inhibition was determined for human P450 isozymes 1A2, 2C9, 2C19, 2D6, and 3A4 by measuring inhibition of each isozyme's ability to process its specific substrate. The assay utilized human liver microsomes (BD Gentest) with the following substrates and incubation times at 37 °C: 1A2: 30 μM phenacetin, 10 min; 2C9: 10 μM diclofenac, 10 min; 2C19: 35 μM *S*-mephenytoin, 45 min; 2D6: 10 μM bufuralol, 10 min; and 3A4: 5 μM midazolam, 5 min. Following incubation samples were analyzed by LC-MS/MS. A range of

test compound concentrations from 0.01 to 10 μM was assayed and IC_{50} values were calculated.

hERG Channel Activity—Assays were conducted to monitor compound effects on the cardiac hERG potassium ion channel, the inhibition of which can result in potentially fatal arrhythmias (43). CHOK1 cells that stably overexpress the hERG ion channel were tested in a whole cell voltage clamp procedure by measuring the ability of a drug to inhibit the peak current flowing through the hERG channel upon depolarization of the membrane potential. Initially, recordings were made in the presence of control saline to establish a baseline (zero inhibition). This was followed by addition of four increasing concentrations of test drug. Each drug was tested in at least three different cells ($n \geq 3$) and the effect of each drug concentration was compared with the baseline to obtain a percent inhibition value. The dose dependent percent inhibition was fitted by a Boltzmann function to generate a dose response curve for the compound and its IC_{50} was determined.

In Vivo Tolerability/Plasma Exposure—In vivo experiments were conducted to gauge tolerability to a range of doses used in subsequent efficacy studies. These studies were also used to gain preliminary data on drug exposure by measuring plasma levels in response to oral dosing. Compounds were dissolved in 5% lactic acid in ethanol then diluted 1:10 with an aqueous solution of 0.9% sodium lactate/10% hydroxypropyl-β-cyclodextrin. Compounds were administered orally twice-daily 8 h apart to groups of 3 female 4 weeks old CD-1 mice at 50, 100 or 200 mg/kg/day in addition to a vehicle control group. Animals were observed every 15 min for the first hr post-dosing, then hourly for 4 h after the first dose for signs of overt toxicity/poor tolerability. Blood was collected at 1 h after the first dose, 1 h before and 1 h after the second dose, and 18 h after the second dose, and plasma levels of compound were determined.

In Vivo Pharmacokinetic Studies—Pharmacokinetic studies on selected compounds were performed in mice, since this is the host species for the *P. berghei* efficacy model. Compounds were formulated as described above. Single-dose studies with both an intravenous arm (5 mg/kg) and an oral arm (10 mg/kg) were performed using 25 g male CD-1 mice with 5 animals/dosing group. At specified intervals (0.083, 0.25, 0.5, 1, 2, 6 and 24 h) blood samples were collected into tubes containing dipotassium EDTA as anti-coagulant for LC/MS/MS analysis to determine concentration of compound. Plasma exposure data were used to generate values for a complete set of pharmacokinetic parameters by non-compartment model using WinNonlin.

In Vivo Efficacy Studies, P. berghei Models—The acute *P. berghei* efficacy model in mice was adapted from Peters' "4-day suppressive test" (44, 45). All initial testing of compounds was conducted at the University of Puerto Rico (UPR), with a limited number of subsequent confirmatory studies performed at the Swiss Tropical and Public Health Institute (Swiss TPH).

The protocol for the studies at UPR was approved by the IACUC of the Medical Sciences Campus, University of Puerto Rico, and all work was conducted in accordance with the "Guide for the Care and Use of Laboratory Animals" and regulations of the PHS Policy on Humane Care and Use of Laboratory Animals (46). Animals were maintained and housed according to NIH guidelines and were allowed to acclimatize for 1 week prior to the commencement of studies. On study day 1, groups of 4–6-week old female Swiss Albino mice (Charles River Laboratories) ($n = 5$) were infected by tail vein injection with 0.2 ml heparinized blood diluted to contain 1×10^7 *P. berghei* N-clone parasites. Compounds were formulated as described above and administered by oral gavage. On study day 1 a single dose was given at 9 h post initial infection, and over the subsequent 3 days the dose was split and administered twice daily, with 6 h between doses. Animals in the Control group received vehicle alone. Dose concentration and frequency of dosing were based upon preliminary exposure and tolerability studies (described above). On study day 5 blood was collected by tail-nick, and thin smear microscope slides were prepared and stained using Diff Quick. A minimum of 300 erythrocytes were counted and the percentage of parasitized erythrocytes was determined. Animals lacking detectable parasites on study day 5 were examined every 2–3 days thereafter to determine whether cure was sterile. Animals with no detectable parasites 28 days after cessation of dosing (study day 32) were considered cured; animals were euthanized at the end of the study.

The *in vivo* studies at the Swiss TPH Institute were performed under a protocol reviewed and approved by the local veterinary authorities of the Canton Basel-Stadt. NMRI mice infected with the ANKA strain MRA-865 (2×10^7 parasites) containing a constitutively-expressed GFP gene (transgenic parasite RMgm-5; http://www.pberghei.eu/index.php?rmgm = 5) (47) were used, in contrast to the Swiss Albino mice and N-strain used at UPR. The protocols followed at the two sites were essentially identical with respect to dosing and timing of parasitemia assessments. Parasitologic assessments were made by resuspending 1 μl tail blood in 1 ml PBS buffer and counting the fluorescent cells in a total of 100,000 erythrocytes using a FACScan (Becton Dickinson). Animals that had no detectable parasites on study day 5 were followed out through study day 30 before being declared cured of infection.

In Vivo Efficacy Studies, P. falciparum Model—Efficacy against *P. falciparum* $Pf3D7^{0087/N9}$ growing in NOD-*scid* IL-$2R\gamma^{null}$ mice engrafted with human erythrocytes was determined as previously described (48). Briefly, groups of 3 animals were infected on day 0 with 2×10^7 parasites. In the test groups, compound was administered twice daily on study days 4–7, while animals in the Control group received no drug. Parasitemia was assessed by FACS as previously described (49).

RESULTS

Identification of Lead Compounds—The N-alkyl-5-(1H-benzimidazol-1-yl)thiophene-2-carboxamides in the present report are analogs derived from Compounds 3 and 4 presented in a previous publication describing a high-throughput screen (25). A manuscript providing details of the analog synthetic pathways and structure-activity relationship is in preparation.

In Vitro Compound Activity—As shown in Table 1, Genz-667348, -668857, and -669178 demonstrated double-digit nanomolar potency against DHODH from *P. falciparum*, *P. berghei* and *P. vivax*, while lacking activity against the human enzyme. These compounds had a profound inhibitory effect on growth of the 3D7 and Dd2 strains of *P. falciparum*, with single-

TABLE 1

***In vitro* activity of DHODH inhibitors**

The abbreviations used are: Pf, *Plasmodium falciparum*; Pb, *Plasmodium berghei*; Pv, *Plasmodium vivax*; Pk, *Plasmodium knowlesi;* Hs, *Homo sapiens.* Results represent the means of duplicate determinations.

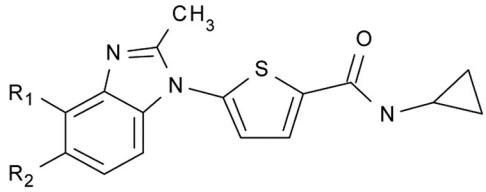

	Substituents		Enzyme Inhibition				Parasite Viability				Human Cell Viability		
Genz-#	R_1	R_2	PfDHODH IC_{50} μM	PbDHODH IC_{50} μM	PvDHODH IC_{50} μM	HsDHODH IC_{50} μM	Pf 3D7 IC_{50} μM	Pf Dd2 IC_{50} μM	Pk IC_{50} μM	Pb IC_{50} μM	Kidney Epithelial LC_{50} μM	Dermal Fibroblast LC_{50} μM	RBC Lysis LC_{50} μM
667348	H	OCF_3	0.022	0.014	0.042	>30	0.007	0.010	0.093	0.091	>62	>62	>40
668857	$OCHF_2$	H	0.044	0.012	0.015	>30	0.019	0.026	0.083	0.084	>62	>62	>40
669178	CN	H	0.050	0.040	0.015	>30	0.008	0.010	Not done	0.068	>62	>62	>40

digit nanomolar IC_{50} values. To determine whether these compounds showed a similar effect on the *in vitro* growth of the rodent parasite *P. berghei*, the *in vitro* susceptibility of blood stages was determined using the *in vitro* drug luminescence assay. Genz-667348 and -668857 both efficiently inhibited the growth of blood stage *P. berghei*, although the IC_{50} values were 5- to 13-fold higher than those obtained for *in vitro* growth inhibition of *P. falciparum*. Due to the interest in treatment and eradication of not just *P. falciparum* malaria but also the *P. vivax*-mediated disease, Genz-667348 and -668857 were assessed for their ability to inhibit the growth of a surrogate parasite, *P. knowlesi*. The IC_{50} values obtained were equivalent to those for inhibition of the growth of *P. berghei*. Finally, these compounds demonstrated a total lack of effect on the viability of human kidney epithelial cells and dermal fibroblasts up to the maximum concentration assayed (62 μM), while also exhibiting no lytic effect on human erythrocytes. These observations provide evidence that the species specificity exhibited for DHODH inhibition correlates with a specific effect on the parasites as compared with representative host cells.

X-ray Structure Determination of Genz-667348 in Complex with PfDHODH—The overall structure of *Pf*DHODH complexed with Genz-667348 (RCSB ID rcsb060790, PDB ID 3O8A) is similar to the previously reported structures of *Pf*DHODH bound to the triazolopyrimidine inhibitors (*e.g.* DSM1) (23) and A77 1726 (50). A short hydrophobic N-terminal helical domain (residues 163–194) precedes a classic β/α barrel domain that begins with β-strand 3 (Fig. 1*A*). The $F_o - F_c$ difference density map showed strong, interpretable density for the bound inhibitor (Genz-667348) between the two N-terminal helices (α1 and α2) and the α/β barrel domain (supplemental Fig. 1S). The inhibitor-binding site is formed adjacent to the FMN site by helices α1 and α2 in the N-terminal extension and helices α3 and α10 and strand β5 in the α/β barrel (Fig. 1, *A* and *B*). The cyclopropyl ring of Genz-667348 contacts β5 and is within Van der Waals distance of the FMN, whereas the trifluoromethoxy group extends toward α1 and α2. The cyclopropyl binds a largely hydrophobic pocket formed by Val-532, Ile-272, and Ile-263. Adjacent to this site are two residues that form the only non-hydrophobic contacts with the inhibitor in the pocket. These include ion pair H-bonds between His-185 and the N of methylformamide, and between Arg-265 and the O of methylformamide. The benzimidazole ring extends toward the protein surface between α1 and α2 and is bound in a hydrophobic pocket formed by Tyr-168, Cys-175, Phe-171, Leu-172, Phe-188, Leu-191, and Leu-531.

Comparison to A77 1726 and DSM1-bound PfDHODH Structures—*Pf*DHODH-348 was superimposed with the structures of *Pf*DHODH bound to A77 1726 (1TV5) and the triazolopyrimidine DSM1 (3I65) with root mean square deviations of 0.7 and 0.6 Å, respectively (Fig. 1*B*). We previously noted that the inhibitor-binding site of *Pf*DHODH is composed of two regions: the H-bond site that contains His-185 and Arg-265, and the hydrophobic pocket (23). The position of the hydrophobic pocket is variable and depends on the conformation of Phe-188, with DSM1 occupying one pocket and A77 1726 occupying the other. These new structures of the enzyme bound to Genz-667348 show that all three inhibitor classes overlap in the H-bond pocket forming interactions with His-185 and Arg-265. Genz-667348 occupies the same hydrophobic pocket as A77 1726 with Phe-188 observed in the up conformation, and thus makes distinct interactions that are not observed in the structures of the enzyme bound to the triazolopyrimidine series of inhibitors. However, as is the case for DSM1, an edge-to-face stacking interaction between Genz-667348 and Phe-188 is present (Fig. 1*B*), suggesting this interaction likely contributes to the potent binding of the inhibitor series. In addition to the previously identified conformational flexibility of Phe-188, the *Pf*DHODH-348 structure demonstrates that Phe-171 is also capable of conformational flexibility. This ring adopts several conformations allowing the protein to accommodate substituents of variable size into the hydrophobic pocket adjacent to this residue.

Comparison to the Human DHODH Structure Bound to Brequinar—To provide insight into the strong species selectivity that is observed for the series, *Pf*DHODH-348 was superim-

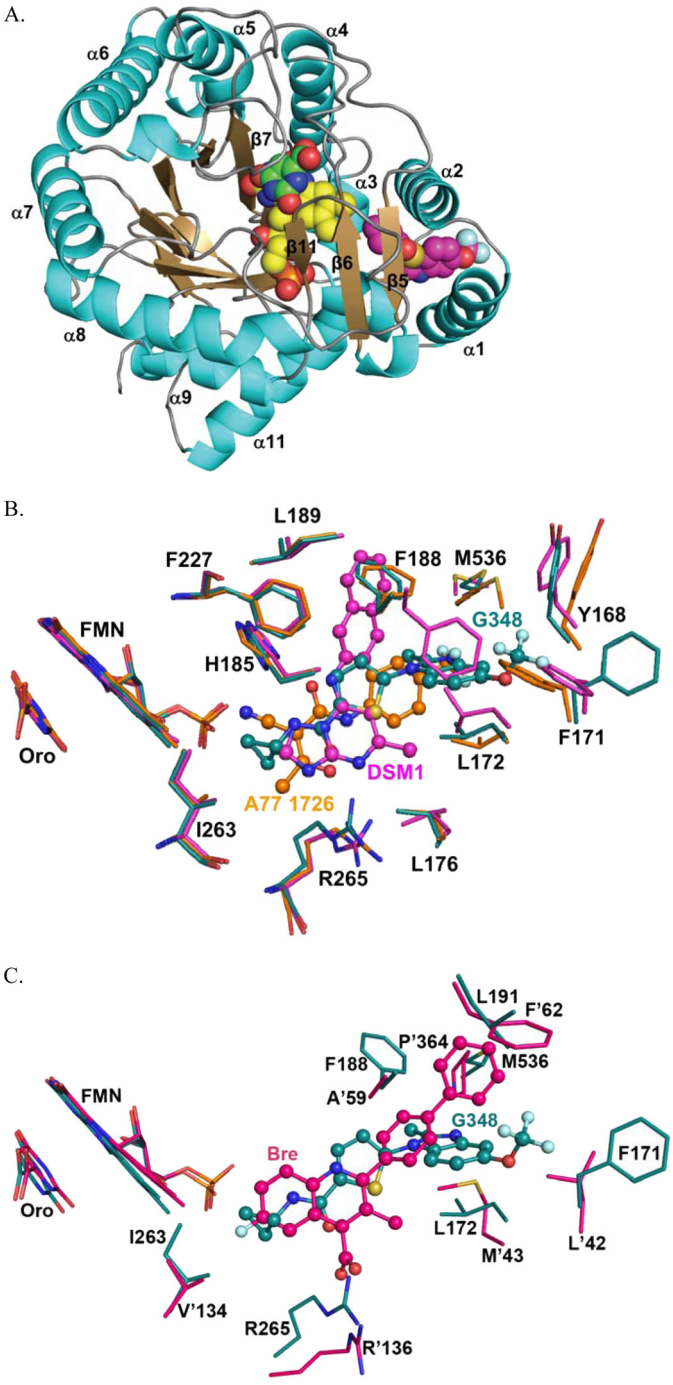

FIGURE 1. **X-ray structure of Genz-667348 in complex with *Pf*DHODH.** *A*, *ribbon diagram* of Genz-667348 bound to *Pf*DHODH. α-Helices are displayed in *teal*, β-strands are displayed in *sand*, ligands are displayed as *space-filling balls*. Atoms are colored as follows: carbon atoms are *yellow* in FMN, *pink* in G348, and *green* in orotate; nitrogen is *blue*; oxygen is *red*; fluorine is *light blue*; and sulfur is *yellow*. *B*, comparison of *Pf*DHODH inhibitor-binding sites. *Pf*DHODH-G348 (*teal*) superimposed with *Pf*DHODH-DSM1 (*pink*) and A77 1726 (*orange*). *Colors* refer to carbon atoms, other atoms are colored as in *A*. Inhibitors are displayed as *balls and sticks*. A subset of residues within 4 Å of the bound inhibitor is displayed. *C*, comparison with the human DHODH inhibitor-binding site. *Pf*DHODH-G348 (*teal*) superimposed with hDHODH-bre (*pink*). Residue numbers for hDHODH are marked with an *apostrophe*, while *Pf*DHODH numbers are not. Inhibitors are displayed as *balls and sticks*.

posed with the structure of human DHODH bound to brequinar (21) (Fig. 1*C*). The two structures superimpose with a root mean square deviation of 1.8 Å. The structural comparison suggests that the selective binding of Genz-667348 to *Pf*DHODH is due to amino acid substitutions in the benzimidazole ring-binding site, including substitution of Leu-46 and Met-43 in human DHODH for Cys-175 and Leu-172 in *Pf*DHODH. The structural alignment suggests that the human residues in these positions overlap the benzimidazole-binding site, providing a structural rationale for the poor inhibition by these compounds of the human enzyme. As noted previously the substitutions of Met-563, Leu-191, and Phe-188 in *Pf*DHODH for Pro-364, Phe-62, and Ala-59 in human DHODH close off the pocket accessed by brequinar and impede binding in the *Pf*DHODH structure (23).

In Vitro Pharmaceutical Properties—The three lead compounds in the *N*-alkyl-5-(1H-benzimidazol-1-yl)thiophene-2-carboxamide series were assessed for a number of *in vitro* drug absorption, distribution, metabolism, and excretion parameters, and the results are presented in Table 2. All three compounds demonstrated moderate solubility (30–50 μg/ml) and good permeability ($>30 \times 10^{-6}$ cm/sec), and they tended to be slightly more hydrophobic than optimal (computed partition coefficient between 3 and 5). Inhibition of cytochrome P450 occurred only for Genz-667348, with inhibition of 2D6 (IC_{50} = 0.1 μM) and to a lesser extent, 2C9 (IC_{50} = 6.2 μM). Intrinsic clearance for these compounds ranged from good to moderate as calculated from experiments using both microsomes and hepatocytes from human, rat, and mouse. Genz-667348 demonstrated hERG channel inhibition, with an IC_{50} value of <2.8 μM. Primarily on the basis of good activity in the *in vitro* enzyme and parasite assays and the prediction of reasonable stability in the mouse, Genz-667348 was selected for advancement into *in vivo* drug metabolism and pharmacokinetics and efficacy studies and evaluation of crystal structure. Two later analogs, Genz-668857 and -669178, exhibited increasingly favorable profiles with respect to cytochrome P450 and hERG inhibition while maintaining good activity, and these compounds were also subjected to further *in vivo* testing.

In Vivo Tolerability/Plasma Exposure—Genz-667348, -668857, and -669178 were administered to mice by oral gavage using twice-daily dosing, and doses up to 200 mg/kg/day elicited no signs of pain, distress, or local or systemic toxicity. Plasma levels of compound were determined, and comparisons with IC_{90} values derived from *in vitro* anti-parasite assays are shown in Fig. 2. Values for area under the curve and plasma compound concentrations at peak and trough are given in Table 3. The values for area under the curve were not significantly different between compounds within a given dose. In addition, the maximum concentrations were similar for all three compounds within a given dose, although the levels for Genz-668857 at 200 mg/kg/day tended to be relatively higher. The most noticeable difference for these compounds was observed in the trough levels, where Genz-667348 at all three doses maintained the highest relative concentrations. At the high dose of 200 mg/kg/day the trough concentration of each compound at 24 h remained above the IC_{90}. For each of these three compounds the exposure data were sufficiently favorable to warrant further *in vivo* testing.

In Vivo Pharmacokinetic Studies—The results of the low dose *in vivo* pharmacokinetic studies are presented in Table 4. All

TABLE 2

DMPK properties of DHODH inhibitors

The abbreviations used are: Sol, solubility; Perm, permeability in PAMPA membranes; CLogP, computed partition coefficient; Micr Clint, intrinsic clearance, microsomal study; Hep Clint, intrinsic clearance, hepatocyte study; H, human, M, mouse. Results represent single determinations.

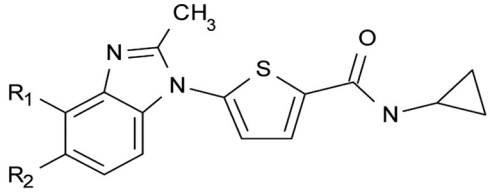

	Substituents		Physical Properties			Cyp Inhibition IC_{50} μM					In Vitro Metabolism							
Genz-#	R_1	R_2	Sol μg/mL	Perm x10^{-6} cm/sec	ClogP	1A2	2C9	2C19	2D6	3A4	Hum Micr Clint ml/min/kg	Rat Micr Clint ml/min/kg	Mouse Micr Clint ml/min/kg	Hum Hep Clint ml/min/kg	Rat Hep Clint ml/min/kg	Mouse Hep Clint ml/min/kg	Plasma Protein Binding % Bound	hERG IC_{50} μM
667348	H	OCF_3	30	81	4.7	>10	6.2	>10	0.1	>10	11	16	83	6	29	<23	H: 98.8 M: 96.7	<2.8
668857	$OCHF_2$	H	50	66	4.1	>10	>10	>10	>10	>10	5	20	51	10	36	18	H: 97.9 M: 90.3	28.8
669178	CN	H	35	39	2.9	>10	>10	>10	>10	>10	<5	<14	34	<5	Not done	36	H: 89.7 M: 66.6	52.9

three compounds exhibited rapid (T_{max} = 0.25–1 h) and efficient (F = 78–145%) oral uptake with comparable values for C_{max} (4.23–6.81 μg/ml). The overall exposure for Genz-667348 appeared to be somewhat greater than the other two compounds as reflected by a higher value for area under the curve, although the half-lives of ~1–3 h for both the intravenous and oral portions of the studies indicated a slightly higher than optimal rate of plasma clearance for all compounds. Clearance was reasonably low with values of 7–18 ml/min/kg, and the values for steady-state volume of distribution (V_{ss}) of 0.45–0.88 liter/kg suggested a uniform distribution throughout the body for each of the compounds.

In Vivo Efficacy Studies, P. berghei Models—Genz-667348, -668857, and -669178 were assessed for *in vivo* efficacy in the 4-day murine *P. berghei* (N-clone) model, and the results are shown in Fig. 3 and Table 5. All three compounds were potent in this animal model, exhibiting ED_{50}, ED_{90}, and ED_{99} values of 13–21 mg/kg/day, 40–56 mg/kg/day, and 108–192 mg/kg/day, respectively. As shown in Fig. 3*A*, Genz-667348 at doses of 100–200 mg/kg/day reduced parasitemia by 99–100%. Because parasitemia may initially be reduced below the limit of microscopic detection even after treatment with sub-curative doses, it is necessary to monitor the levels of parasites in the blood following cessation of dosing, determining the first day at which parasites again become detectable (recrudescence). Animals that have no detectable parasites through day 30 are deemed cured. The results are typically presented in a Kaplan-Meyer plot, following recrudescence for a given population as a function of dose over time. As shown in Fig. 3*B*, Genz-667348 reduced parasitemia to undetectable levels in 3 of 5 mice at day 5, with recrudescence occurring by day 9. At a dose of 200 mg/kg/day parasitemia was undetectable in all 5 animals at day 5, with recrudescence occurring by day 15. Genz-668857 and -669178 were only dosed to a maximum of 100 mg/kg/day, at which level measurable parasitemia existed in all animals at day 5 (0.4 ± 0.2% and 1.6 ± 1.1%, respectively). As a result, there was no recrudescence study phase for these two compounds.

One compound, Genz-667348, was chosen for evaluation in a mouse efficacy model using the ANKA strain of *P. berghei*. The results of this study are shown in Fig. 4 and Table 5. The values for ED_{50}, ED_{90}, and ED_{99} were 3- to 4-fold lower than the corresponding values obtained in the N-clone study, suggesting a greater potency against the ANKA strain. A Kaplan-Meyer plot showing the onset of recrudescence as a function of dose is shown in Fig. 4*B*, with a clear indication that the length of time for relapse was proportional to the dose of compound administered. Of particular importance is the fact that sterile cure was achieved in this model at a dose of 100 mg/kg/day, as defined by a failure for recrudescence to occur within thirty days after infection.

In Vivo Efficacy Studies, P. falciparum Model—Genz-667348 was tested for efficacy against *P. falciparum* $Pf3D7^{0087/N9}$ growing in NOD-*scid* IL-$2R\gamma^{null}$ mice engrafted with human erythrocytes, and the results are shown in Table 5. The values for ED_{50}, ED_{90}, and ED_{99} were similar to the corresponding values derived from the *P. berghei* studies, and they were virtually identical to those from the ANKA strain study. These results are important in that they demonstrate direct activity for the compound against the human parasite rather than a surrogate organism. The similarity of the results for the two species of *Plasmodium* provides additional validation for use of the *P. berghei* rodent model as a tool for discovery of agents to treat the human disease.

DISCUSSION

Malaria is one of the world's most devastating endemic diseases, particularly in developing countries, and there is an acute need for new therapeutic approaches because of rapidly increasing resistance to current pharmaceutics. DHODH is a critical enzyme for survival of the parasite, and it represents a potential target for an anti-malarial therapy, as indicated by several reports in the literature. The importance of the target is underscored by the fact that multiple unique chemical series are currently undergoing lead optimization programs. Phillips *et al.* described a promising series of triazolopyrimidine compounds with inhibitory activity against the enzyme and potency against the parasite both *in vitro* and in animal models (26, 27). The screening campaign performed at Genzyme and the Broad

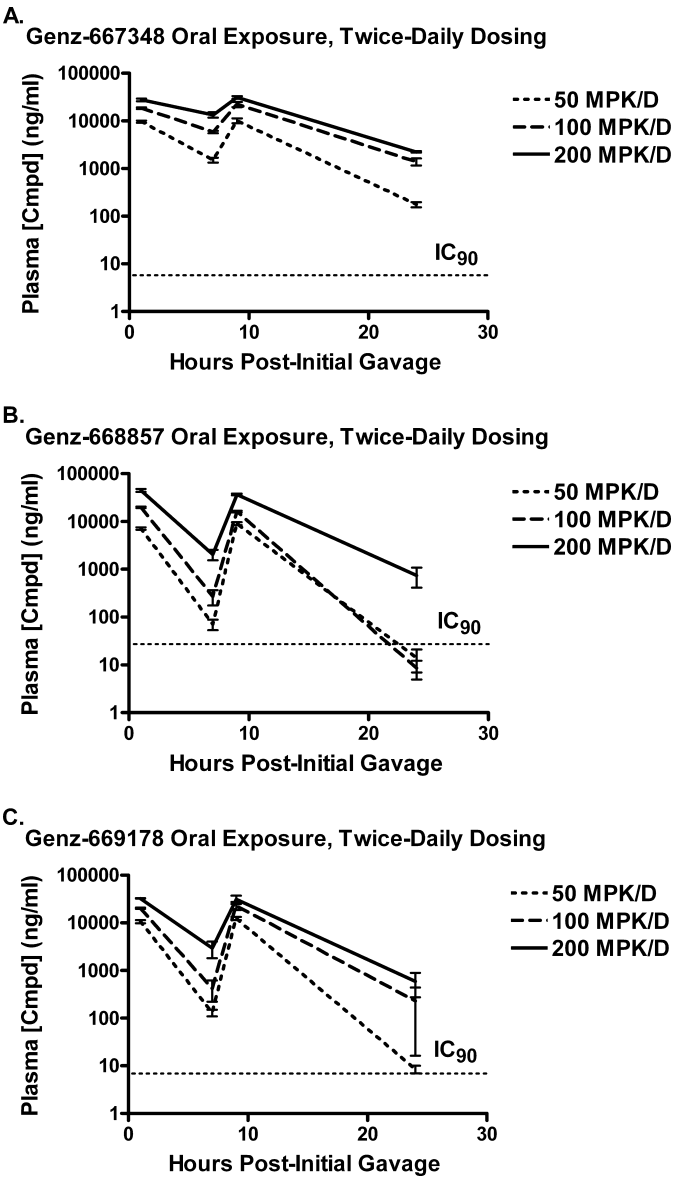

FIGURE 2. **Oral exposure of DHODH inhibitors in the mouse.** Genz-667348 (*A*), -668857 (*B*), and -669178 (*C*) were administered to mice by oral gavage using twice daily dosing for a single day, and plasma samples were collected over a 24-h period for analysis as described under "Experimental Procedures." Exposure levels are shown relative to the IC_{90} values derived from *in vitro* parasite viability studies. Results represent the means for three animals per dose ± S.D.

Institute and described previously identified several additional diverse chemical scaffolds with activity against the enzyme (25), the most promising of which is the *N*-alkyl-5-(1H-benzimidazol-1-yl)thiophene-2-carboxamide series described in the current report. Data presented here demonstrate that these compounds are highly potent DHODH inhibitors, possess comparable activity in a parasite viability assay, exhibit favorable drug metabolism and pharmacokinetics properties, and are efficacious in animal models of the disease. In particular, sterile cure was achieved in the *P. berghei* ANKA strain mouse model with the compound Genz-667348, which to the best of our knowledge is the first evidence of this effect with a plasmodial DHODH inhibitor.

Potency against both the enzyme and the parasite was highly correlated throughout this compound class. Previous studies on the original indole screen hit (Genz-582463) and some closely related analogs using a transgenic strain of *P. falciparum* expressing DHODH from *S. cerevisiae* confirmed inhibition of this enzyme as the primary mode of action (25), and this finding is currently being confirmed for several later benzimidazole analogs, including those described herein. The interaction between one of the most potent analogs, Genz-667348, and *Pf*DHODH was elucidated by crystallography. The x-ray structure of the enzyme-inhibitor complex reveals extensive contacts, consistent with the observed potent binding of the series. Conformational flexibility allows Genz-667348 to access an alternative hydrophobic pocket from the triazolopyrimidines (*e.g.* DSM1), enabling the enzyme to bind two alternative chemical scaffolds with high potency. The structural flexibility enhances the value of *Pf*DHODH as a drug target by expanding the chemical space that can be evaluated for the discovery of suitable inhibitors with the potential to lead to drugs.

The species selectivity of this series was evaluated and showed that these compounds also inhibited DHODH from *P. berghei* and *P. vivax*, important in the first instance for validation of the animal model and in the second instance for the potential development of a candidate with pan-parasite activity. In addition, whereas activity against the parasite enzymes translated into toxicity against their respective organisms, there was no effect on the human enzyme. The structural basis for this species selectivity is evident from the co-crystal structure of *Pf*DHODH with Genz-667348. The requirement for an accelerated *de novo* synthesis of pyrimidines in certain rapidly divid-

TABLE 3

Plasma exposure in mice

Abbreviations are: AUC, area under the curve; C_{max1}, concentration at 1 h (1 h post initial dose); C_{max2}, concentration at 9 h (1 h post second dose); $C_{trough1}$, concentration at 7 h (1 h pre second dose); $C_{trough2}$, concentration at 24 h. Results represent the means (S.D.) of results obtained from five animals/group.

	AUC	C_{max1}	C_{max2}	$C_{trough1}$	$C_{trough2}$
	*h*μg/ml*	*ng/ml*	*ng/ml*	*ng/ml*	*ng/ml*
200 mg/kg/day					
Genz-667348	418 (53)	27694 (3140)	31116 (3696)	13447 (3054)	2235 (124)
Genz-668857	460 (22)	44804 (5238)	36736 (2511)	2035 (870)	747 (579)
Genz-669178	378 (99)	32519 (612)	31134 (10793)	2927 (1922)	586 (539)
100 mg/kg/day					
Genz-667348	279 (46)	18511 (1424)	22324 (4796)	5859 (550)	1394 (423)
Genz-668857	198 (8)	19763 (1044)	16243 (1222)	271 (167)	9 (6)
Genz-669178	259 (68)	20199 (973)	23035 (7765)	419 (345)	229 (367)
50 mg/kg/day					
Genz-667348	122 (13)	9691 (1005)	10095 (2058)	1513 (310)	177 (37)
Genz-668857	98 (12)	7099 (761)	9061 (1127)	70 (31)	14 (12)
Genz-669178	137 (12)	10631 (1318)	12385 (1649)	130 (35)	9 (3)

TABLE 4

Pharmacokinetic properties in mice

Abbreviations are: T_{max}, time to maximum compound concentration; C_{max}, maximum compound concentration; $T_{½}$, terminal half-life of the compound; AUC_{last}, area under the curve to last quantifiable concentration; AUC_{INF}, area under the curve extrapolated to infinite time; *F*, % of compound orally bioavailable; CL, calculated rate of clearance from plasma; V_{SS}, steady-state volume of distribution. The results were derived from curves incorporating data from five animals/compound.

Genz#	10 MPK Oral						5 MPK Intravenous		
	T_{max}	C_{max}	$T_{½}$	AUC_{last}	AUC_{INF}	*F*	CL	V_{SS}	$T_{½}$
	h	*μg/ml*	*h*	*h*μg/ml*	*h* μg/ml*	*%*	*ml/min/kg*	*liters/kg*	*h*
667348	0.50	5.22	1.92	35.10	35.10	145	6.9	0.88	1.67
668857	0.25	6.81	3.20	14.00	14.00	78	9.3	0.45	1.83
669178	1.00	4.23	1.00	9.40	9.50	102	18.0	0.71	0.73

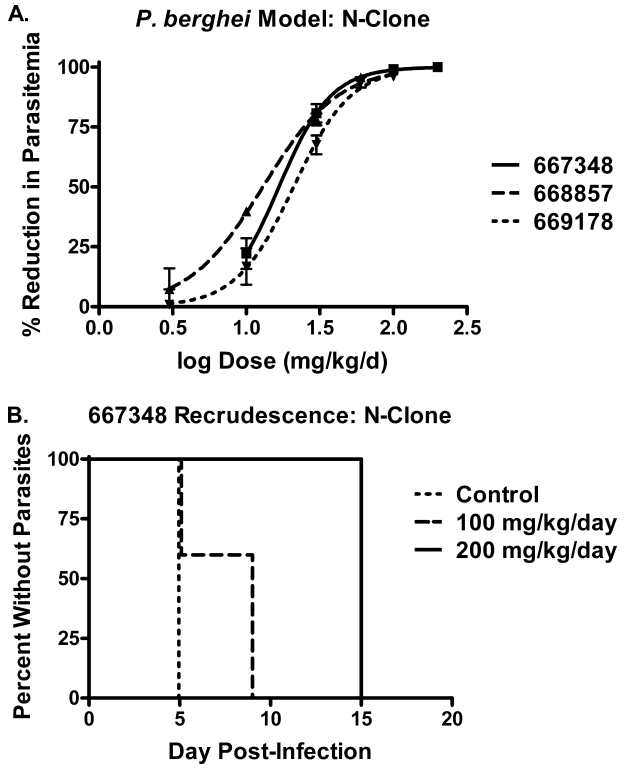

FIGURE 3. **Compound efficacy in the *P. berghei* mouse model (N-clone).** Animals were dosed once on day 1 and with split twice daily dosing on days 2–4. *A*, reduction in parasitemia for Genz-667348, -668857, and -669178 as a function of dose. ED_{50} values: 667348, 16.7 mg/kg/day; 668857, 13.0 mg/kg/day; and 669178, 21.0 mg/kg/day. Results represent the means for five animals per dose ± S.D. *B*, Kaplan-Meyer plot demonstrating the effect of dose of Genz-667348 on time to recrudescence. The high dose of 200 mg/kg/day delayed the reappearance of parasites until day 15; a sterile cure was not achieved.

ing human cells such as activated lymphocytes (51) makes it desirable to identify compounds specific for the parasite DHODH, and the opportunity to achieve an adequate therapeutic window appears to be excellent.

The compounds in this series differed in their *in vitro* drug metabolism and pharmacokinetics properties, most notably with regard to cytochrome P450 inhibition. Because of rapidly evolving resistance, anti-malarials are unlikely to be administered as monotherapy, with the result that drug-drug interactions are an important consideration. Cytochromes 2C9 and 2D6 were the most likely isozymes to be affected by the compounds described herein, and a number of substrates and inducers across several compound classes have been described for both (52). However, neither cytochrome P450 plays a significant role in the disposition of anti-malarials (53), so issues would primarily concern other co-therapies. Nevertheless, a number of analogs in this compound series exhibited an absence of activity against these enzymes, and the ultimate goal would be the selection of a candidate with little to no cytochrome P450 inhibition.

The DHODH inhibitors in this report exhibited variability with regard to metabolic stability predicted from studies with microsomes and hepatocytes. The earliest compound in this series to undergo *in vivo* testing, Genz-667348, was chosen primarily on the basis of good activity against both the enzyme and the parasite along with the prediction of reasonable stability. Although potent, this compound produced significant inhibition of CYP2D6 as well as the cardiac hERG channel, rendering it somewhat less desirable as a development candidate. Later analogs, Genz-668857 and -669178, were selected on the basis of equivalent activity, and more favorable cytochrome P450 and hERG inhibition properties when compared with Genz-667348. Exposure studies monitoring plasma levels of compound for 24 h after twice daily dosing demonstrated that each compound maintained plasma levels above the IC_{90} for the entire study period, and pharmacokinetic studies indicated that each compound was readily taken up into plasma and maintained a reasonable residence time. Tolerability was excellent at all doses tested (up to 200 mg/kg/day), and the compounds were carried forward into efficacy studies.

Genz-667348, -668857, and -669178 underwent testing in the murine *P. berghei* N-clone model and demonstrated similar potencies, with ED_{50} values of 13–21 mg/kg/day. In this model, chloroquine and artemisinin are curative at 30 and 100 mg/kg/day, respectively (data not shown). Genz-667348 was further studied in the murine *P. berghei* ANKA strain model, and sterile cure was achieved following 4 days of twice daily dosing for a total dose of 100 mg/kg/day. To the best of our knowledge this is the first report of sterile cure in a murine model in response to treatment with an inhibitor of DHODH. It is interesting that sterile cure was achieved when the infecting parasite was the ANKA strain of *P. berghei* but not the N-clone, although it is conceivable that higher concentrations or longer treatment would have yielded cure in the latter model as well. Genz-667348 did demonstrate a 3- to 4-fold greater *in vitro* potency against the ANKA strain as compared with the N-clone, and this difference may be substantial enough to account for the selective cure. Alternatively, the difference in the susceptibility of the parasites may lie in differences between the original source of these isolates or in the laboratory history of these lines. The N-clone has been derived from the K173 strain that has been kept in the

TABLE 5

***In vivo* efficacy in mouse models**

Efficacy values expressed as mg/kg/day. In *P. berghei* N-clone studies (University of Puerto Rico) animals were dosed once on day 1 and with split twice daily dosing on days 2–4. In *P. berghei* ANKA strain studies (Swiss Tropical and Public Health Institute) animals were dosed twice daily. In the *P. falciparum* study (GlaxoSmithKline) NOD-*scid* IL-2Rγ^{null} mice were engrafted with human erythrocytes, and animals were dosed twice daily. ED_{50} values were derived from dose-response curves incorporating data from five animals/group. ED_{90} and ED_{99} values were calculated from ED_{50} values and slopes of the curves using GraphPad software.

	Genz-667348			Genz-668857			Genz-669178		
	ED_{50}	ED_{90}	ED_{99}	ED_{50}	ED_{90}	ED_{99}	ED_{50}	ED_{90}	ED_{99}
					mg/kg/day				
P. berghei N	16.7	40.9	108.7	13.0	47.1	192.3	21.0	56.5	165.9
P. berghei ANKA	6.1	12.7	28.3	ND[a]	ND	ND	ND	ND	ND
P. falciparum 3D7$^{0087/N9}$	5.3	11.0	24.5	ND	ND	ND	ND	ND	ND

[a] ND, not determined.

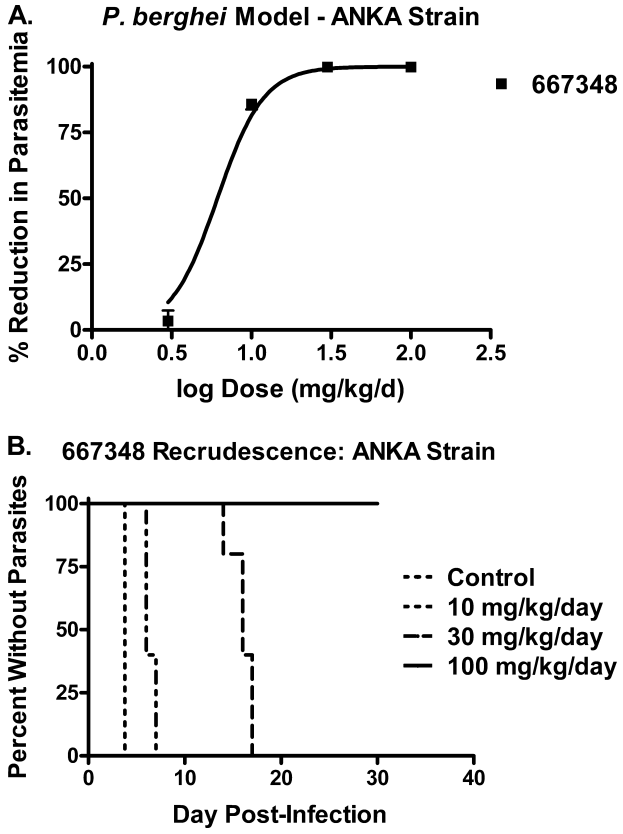

FIGURE 4. **Efficacy of Genz-667348 in the *P. berghei* mouse model (ANKA strain).** Animals were dosed twice daily. *A*, reduction in parasitemia for Genz-667348 as a function of dose. ED_{50} value: 6.1 mg/kg/day. Results represent the means for five animals per dose ± S.D. *B*, Kaplan-Meyer plot demonstrating the effect of dose of Genz-667348 on time to recrudescence. A sterile cure was achieved at 4 days of twice daily dosing at 100 mg/kg/day.

laboratory by mechanical passage for prolonged periods (54), whereas the lines of the ANKA strain are derived from the original ANKA isolate (55). The causes of the different response to DHODH inhibitors in the two lines are yet unknown, but plans are in place to incorporate the ANKA strain model into the assay cascade.

The efficacy of the compounds described in this report is particularly encouraging in light of the fact that any inhibitor of DHODH developed for use in humans would most probably represent one portion of a combination therapy. Because the approach being utilized for these compounds is inhibition of an enzyme crucial for the viability of the parasite, the development of resistance, potentially via mutation of the enzyme, is a possibility. For this reason resistance selection studies are underway on the lead compounds from this series. Nevertheless, evidence of sterile cure in the mouse with a compound from this series used as a monotherapy suggests that DHODH inhibition should be a valuable addition to anti-malarial strategies.

In conclusion, we have demonstrated that the *N*-alkyl-5-(1H-benzimidazol-1-yl)thiophene-2-carboxamide series offers a potential scaffold for the development of anti-malarial agents. These compounds derive from an iterative medicinal chemistry program, which originated with a high throughput screen of 215,000 diverse compounds contained within the Genzyme library, and they represent novel structures not previously described for this application. Further refinement of the structure-activity relationship within this series is underway, with Genz-668857 and -669178 undergoing further testing to determine if they represent suitable candidates for preclinical development. In addition, the search for closely related compounds representing distinct new scaffolds with anti-DHODH activity is currently ongoing.

Acknowledgment—We thank Dr. Leonard D. Shultz and The Jackson Laboratory for providing access to NSG mice.

REFERENCES

1. Subbayya, I. N., Ray, S. S., Balaram, P., and Balaram, H. (1997) *Indian J. Med. Res.* **106,** 79–94
2. Reyes, P., Rathod, P. K., Sanchez, D. J., Mrema, J. E., Rieckmann, K. H., and Heidrich, H. G. (1982) *Mol. Biochem. Parasitol.* **5,** 275–290
3. Caroline, D. F. (1969) *J. Bacteriol.* **100,** 1371–1377
4. Taylor, M. L., Taylor, W. H., Eames, D. F., and Taylor, C. D. (1971) *J. Bacteriol.* **105,** 1015–1027
5. Williams, J. C., and O'Donovan, G. A. (1973) *J. Bacteriol.* **115,** 1071–1076
6. Jones, M. E. (1980) *Annu. Rev. Biochem.* **49,** 253–279
7. van der Plas, J., Hellingwerf, K. J., Seijen, H. G., Guest, J. R., Weiner, J. H., and Konings, W. N. (1983) *J. Bacteriol.* **153,** 1027–1037
8. Skophammer, R. G., Servin, J. A., Herbold, C. W., and Lake, J. A. (2007) *Mol. Biol. Evol.* **24,** 1761–1768
9. Denis-Duphil, M. (1989) *Biochem. Cell Biol.* **67,** 612–631
10. Jordan, D. B., Bisaha, J. J., and Picollelli, M. A. (2000) *Arch. Biochem. Biophys.* **378,** 84–92
11. Chen, J. J., and Jones, M. E. (1976) *Arch. Biochem. Biophys.* **176,** 82–90
12. Gero, A. M., O'Sullivan, W. J., and Brown, D. J. (1985) *Biochem. Med.* **34,** 60–69
13. Knecht, W., and Löffler, M. (1998) *Biochem. Pharmacol.* **56,** 1259–1264
14. Taylor, W. H., and Taylor, M. L. (1964) *J. Bacteriol.* **88,** 105–110
15. Löffler, M., Jöckel, J., Schuster, G., and Becker, C. (1997) *Mol. Cell Biochem.* **174,** 125–129
16. Eakin, R. T., and Mitchell, H. K. (1969) *Arch. Biochem. Biophys.* **134,** 160–171
17. Kennedy, J. (1973) *Arch. Biochem. Biophys.* **157,** 369–373
18. Miller, R. W., and Curry, J. R. (1969) *Can J. Biochem.* **47,** 725–734

19. Fry, M., and Beesley, J. E. (1991) *Parasitology* **102,** 17–26
20. Painter, H. J., Morrisey, J. M., Mather, M. W., and Vaidya, A. B. (2007) *Nature* **446,** 88–91
21. Liu, S., Neidhardt, E. A., Grossman, T. H., Ocain, T., and Clardy, J. (2000) *Structure* **8,** 25–33
22. Hurt, D. E., Sutton, A. E., and Clardy, J. (2006) *Bioorg. Med. Chem. Lett.* **16,** 1610–1615
23. Deng, X., Gujjar, R., El Mazouni, F., Kaminsky, W., Malmquist, N. A., Goldsmith, E. J., Rathod, P. K., and Phillips, M. A. (2009) *J. Biol. Chem.* **284,** 26999–27009
24. Baldwin, J., Farajallah, A. M., Malmquist, N. A., Rathod, P. K., and Phillips, M. A. (2002) *J. Biol. Chem.* **277,** 41827–41834
25. Patel, V., Booker, M., Kramer, M., Ross, L., Celatka, C. A., Kennedy, L. M., Dvorin, J. D., Duraisingh, M. T., Sliz, P., Wirth, D. F., and Clardy, J. (2008) *J. Biol. Chem.* **283,** 35078–35085
26. Phillips, M. A., Gujjar, R., Malmquist, N. A., White, J., El Mazouni, F., Baldwin, J., and Rathod, P. K. (2008) *J. Med. Chem.* **51,** 3649–3653
27. Gujjar, R., Marwaha, A., El Mazouni, F., White, J., White, K. L., Creason, S., Shackleford, D. M., Baldwin, J., Charman, W. N., Buckner, F. S., Charman, S., Rathod, P. K., and Phillips, M. A. (2009) *J. Med. Chem.* **52,** 1864–1872
28. Otwinowski, Z., and Minor, W. (1997) *Methods Enzymol.* **276,** 307–326
29. McCoy, A. J. (2007) *Acta Crystallogr. D Biol. Crystallogr.* **63,** 32–41
30. Emsley, P., and Cowtan, K. (2004) *Acta Crystallogr. D Biol. Crystallogr.* **60,** 2126–2132
31. Murshudov, G. N., Vagin, A. A., and Dodson, E. J. (1997) *Acta Crystallogr. D Biol. Crystallogr.* **53,** 240–255
32. Cowtan, K. (1998) *Acta Crystallogr. D Biol. Crystallogr.* **54,** 750–756
33. Davis, I. W., Leaver-Fay, A., Chen, V. B., Block, J. N., Kapral, G. J., Wang, X., Murray, L. W., Arendall, W. B., 3rd, Snoeyink, J., Richardson, J. S., and Richardson, D. C. (2007) *Nucleic Acids Res.* **35,** W375–W383, web server issue
34. Kleywegt, G. J., and Jones, T. A. (1994) *CCP4/ESF-EACBM Newsletter on Protein Crystallography* **31,** 9–14
35. Holm, L., and Park, J. (2000) *Bioinformatics* **16,** 566–567
36. Plouffe, D., Brinker, A., McNamara, C., Henson, K., Kato, N., Kuhen, K., Nagle, A., Adrián, F., Matzen, J. T., Anderson, P., Nam, T. G., Gray, N. S., Chatterjee, A., Janes, J., Yan, S. F., Trager, R., Caldwell, J. S., Schultz, P. G., Zhou, Y., and Winzeler, E. A. (2008) *Proc. Natl. Acad. Sci. U.S.A.* **105,** 9059–9064
37. Kocken, C. H., Ozwara, H., van der Wel, A., Beetsma, A. L., Mwenda, J. M., and Thomas, A. W. (2002) *Infect. Immun.* **70,** 655–660
38. Franke-Fayard, B., Djokovic, D., Dooren, M. W., Ramesar, J., Waters, A. P., Falade, M. O., Kranendonk, M., Martinelli, A., Cravo, P., and Janse, C. J. (2008) *Int. J. Parasitol.* **38,** 1651–1662
39. Janse, C. J., and Waters, A. P. (1995) *Parasitol. Today* **11,** 138–143
40. Janse, C. J., Franke-Fayard, B., Mair, G. R., Ramesar, J., Thiel, C., Engelmann, S., Matuschewski, K., van Gemert, G. J., Sauerwein, R. W., and Waters, A. P. (2006) *Mol. Biochem. Parasitol.* **145,** 60–70
41. Kansy, M., Senner, F., and Gubernator, K. (1998) *J. Med. Chem.* **41,** 1007–1010
42. Obach, R. S., Baxter, J. G., Liston, T. E., Silber, B. M., Jones, B. C., MacIntyre, F., Rance, D. J., and Wastall, P. (1997) *J. Pharmacol. Exp. Ther.* **283,** 46–58
43. Sanguinetti, M. C., and Tristani-Firouzi, M. (2006) *Nature* **440,** 463–469
44. Peters, W. (1975) *Ann. Trop. Med. Parasitol.* **69,** 155–171
45. Peters, W. (1987) *Chemotherapy and Drug Resistance in Malaria*, 2nd Ed., pp. 145–273, Academic Press, Orlando, FL
46. National-Research-Council. (1996) *Guide for the Care and Use of Laboratory Animals*, National Academy Press, Washington, D. C.
47. Franke-Fayard, B., Trueman, H., Ramesar, J., Mendoza, J., van der Keur, M., van der Linden, R., Sinden, R. E., Waters, A. P., and Janse, C. J. (2004) *Mol. Biochem. Parasitol.* **137,** 23–33
48. Angulo-Barturen, I., Jiménez-Díaz, M. B., Mulet, T., Rullas, J., Herreros, E., Ferrer, S., Jiménez, E., Mendoza, A., Regadera, J., Rosenthal, P. J., Bathurst, I., Pompliano, D. L., Gómez de las Heras, F., and Gargallo-Viola, D. (2008) *PLoS ONE* **3,** e2252
49. Jiménez-Díaz, M. B., Mulet, T., Gómez, V., Viera, S., Alvarez, A., Garuti, H., Vázquez, Y., Fernández, A., Ibáñez, J., Jiménez, M., Gargallo-Viola, D., and Angulo-Barturen, I. (2009) *Cytometry A* **75,** 225–235
50. Hurt, D. E., Widom, J., and Clardy, J. (2006) *Acta Crystallogr. D Biol. Crystallogr.* **62,** 312–323
51. Fairbanks, L. D., Bofill, M., Ruckemann, K., and Simmonds, H. A. (1995) *J. Biol. Chem.* **270,** 29682–29689
52. Hersh, E. V., and Moore, P. A. (2004) *J. Am. Dent. Assoc.* **135,** 298–311
53. Giao, P. T., and de Vries, P. J. (2001) *Clin. Pharmacokinet.* **40,** 343–373
54. Saul, A., Prescott, N., Smith, F., Cheng, Q., and Walliker, D. (1997) *Mol. Biochem. Parasitol.* **84,** 143–147
55. Janse, C. J., Ramesar, J., and Waters, A. P. (2006) *Nat. Protoc.* **1,** 346–356
56. DeLano, W. L. (2002) *The PyMOL Molecular Graphics System*, DeLano Scientific LLC, San Carlos, CA